PCCP

RSC Publishing

PAPER

View Article Online
View Journal | View Issue

Cite this: *Phys. Chem. Chem. Phys.*, 2013, **15**, 7679

Synthesis and optical characterisation of triphenylamine-based hole extractor materials for CdSe quantum dots†

Miquel Planells,‡[a] Luke X. Reynolds,‡[b] Umesh Bansode,[c] Shraddha Chhatre,[c] Satishchandra Ogale,[c] Neil Robertson*[a] and Saif A. Haque*[b]

Received 5th March 2013,
Accepted 9th April 2013

DOI: 10.1039/c3cp50980j

www.rsc.org/pccp

We report the synthesis and optical characterisation of different triphenylamine-based hole capture materials able to anchor to CdSe quantum dots (QDs). Cyclic voltammetry studies indicate that these materials exhibit reversible electrochemical behaviour. Photoluminescence and transient absorption spectroscopy techniques are used to study interfacial charge transfer properties of the triphenylamine functionalized CdSe QDs. Specifically, we show that the functionalized QDs based on the most easily oxidised triphenylamine display efficient hole-extraction and long-lived charge separation. The present findings should help identify new strategies to control charge transfer QD-based optoelectronic devices.

1. Introduction

Semiconductor quantum dots (QDs) have attracted much recent interest due to their outstanding optical properties and potential application in several fields including biomedical diagnosis and energy conversion systems.[1,2] Nowadays, semiconductor nanocrystals can be produced from various synthetic procedures giving good control over their size, shape and surface coverage, which all ultimately define both the optical and electrochemical properties of the QDs and facilitate their tuneability. In photovoltaic devices, QDs have been applied successfully in a wide range of architectures such as the bulk heterojunction,[3] and in dye-sensitised solar cells (DSSCs).[4]

Recent studies have shown that one of the main limitations on charge yields within QD-based DSSCs is fast recombination of the photogenerated electron and hole due to their constrained spatial separation, possibly accentuated by the fact that the electron injection step can be slower than the hole transfer.[5,6] Consequently, there is a need to develop research strategies that address both the understanding of the mechanisms of such hole transfer processes, and provide potential routes to overcome their limitations. One strategy we are pursuing to tackle both of these themes is to design efficient hole extractor materials that can be attached to the surface of the QDs. The rationale behind such materials is that they could quickly move the photogenerated hole away from the surface of the QD thus giving the electron more time to inject and so potentially overcome the transfer-rate limitation, while at the same time facilitating its study. To achieve this, we have attached electron-donating ligands onto the surface of the QDs in order to facilitate rapid extraction of the hole from the QDs, thus spatially separating it from the electron and retarding the recombination process.

Here, we report three hole-capture molecules based upon triphenylamine (TPA) units with different electron-donating groups attached (Fig. 1). TPA units are well known not only as emissive and hole-transporter materials in electroluminescent devices but also for their ability to accept holes without degradation due to reversible electrochemical behaviour. In this regard, our new molecules differ fundamentally from typical surface ligands for QDs such as thiols, amines, acids or phosphine oxides which, although electron donating, cannot act as stable and reversible hole acceptors. The new molecules also possess a protected thiol which allows them to anchor to the surface of CdSe QDs. Finally, an acetylene group is attached as a bridge between the TPA and protected thiol group moieties

[a] *EastChem School of Chemistry, University of Edinburgh, West Mains Road, Edinburgh, EH9 3JJ, UK. E-mail: neil.robertson@ed.ac.uk; Tel: +44 (0)131 650 4755*

[b] *Department of Chemistry and Centre for Plastics Electronics, Imperial College London, SW7 2AZ, UK. E-mail: s.a.haque@imperial.ac.uk; Tel: +44 (0)207 594 1886*

[c] *Physical and Materials Chemistry Division, National Chemistry Laboratory (CSIR-NCL), Pune-411008, India. E-mail: sb.ogale@ncl.res.in; Tel: +91 20 2590 2260*

† Electronic supplementary information (ESI) available: Powder XRD of CdSe QDs. Cyclic voltammetry at different scan rates and differential pulse voltammetry of neat TPA derivatives. Single-photon counting fitting. Transient absorption spectrum. Reorganisation energies table. See DOI: 10.1039/c3cp50980j

‡ These authors contributed equally to this work.

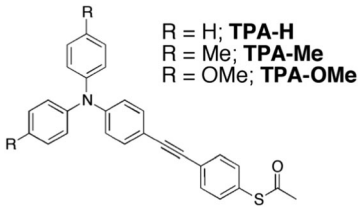

Fig. 1 Molecular structure of thiol-protected triphenylamine (TPA) based materials used in this study.

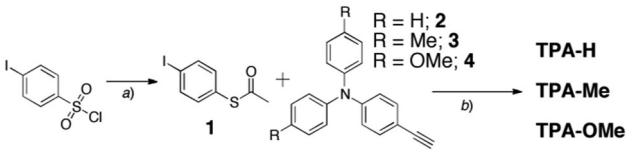

Scheme 1 Synthesis of thiol-protected TPA derivatives. Reaction conditions (a) (i) Me_2SiCl_2, dimethylacetamide, Zn powder, CH_2Cl_2, (ii) AcCl; (b) $(PPh_3)_2PdCl_2$, CuI, triethylamine, THF.

to provide good electronic coupling for efficient hole extraction. We have studied these systems with a range of spectroscopy techniques in solution in order to monitor their optical behaviour as well as the interfacial structure–function relationship.

2. Results and discussion

Oleic acid capped CdSe quantum dots (from here on referred to simply as the CdSe QDs) were synthesized by the hot injection method as described in the experimental section. The HR-TEM images show uniform distribution of spherical CdSe quantum dots with a diameter of around 4–5 nm (Fig. 2). The lattice fringes reveal the crystalline nature of CdSe QDs with a *d*-spacing of 0.35 nm (111) which matches well with that for CdSe. The selected area electron diffraction (SAED) image clearly shows diffused rings as expected for extremely tiny nanoparticles. The innermost ring in the SAED corresponds to the (111) plane with highest *d*-value of 0.35 nm. The powder X-ray diffraction pattern shows the pure phase nature of CdSe QDs (ESI†). The diffraction peaks are broad and all of them match with the zincblende structure of CdSe QDs.[7] Based on Scherrer's equation the nanoparticles exhibit a mean diameter of about 4–5 nm, consistent with the HR-TEM data.

TPA derivatives have been synthesised according to Scheme 1. Terminal acetylene precursors were synthesized following the procedure described previously by our group. Protected thiol precursor **1** was attained by a reduction of pipsyl chloride with Zn metal.[8] It is worth noting that the thiol group must be protected before carrying out the Sonogashira cross-coupling reaction, and therefore protected TPA derivatives were obtained. Unprotected thiols can also be obtained afterwards but they are prone to oxidation in air and hard to handle. Therefore, this study was carried out using protected thiols as explained later in this text.

Table 1 Summary of the optical and electronic properties of isolated molecules used in this study

	λ_{max}/nm	λ_{em}[a]/nm	E_{gap}[b]/eV	E_{HOMO}[c]/eV	$E_{excited\ state}$[d]/eV
TPA-H	362	445	3.10	−5.37	−2.27
TPA-Me	367	472	3.02	−5.17	−2.15
TPA-OMe	368	512	2.89	−4.99	−2.10
CdSe QDs	535	570	2.22	−5.74[e]	−3.41[e]

[a] Excited at 365 nm. [b] From the intersection of absorption and emission spectra. [c] DPV measured from 0.1 M [TBA][PF_6] in CH_2Cl_2 and referenced to ferrocene. E_{HOMO} (eV) = −1.4 E_{CV} (V) −4.6.[11] [d] $E_{excited\ state} = E_{HOMO} + E_{gap}$. [e] The data were obtained from the literature.[22]

Optical and electronic properties of the neat TPA derivatives were studied in detail and are displayed in Table 1. The absorption maximum is located in the UV region with a high molar absorption ($\varepsilon \sim 4 \times 10^4$ cm^{-1} M^{-1}), which does not differ greatly with the substituent on the TPA moiety. However, we observe a clear red-shift in the photoluminescence as the electron-donating ability increases (Fig. 3). This shift could be explained as an effective singlet excited state energy stabilization due to the presence of electron-donating units.[9,10] As expected, by increasing the electron-donating character of the substituent on the TPA derivatives (–H < –Me < –OMe) a marked shift in the oxidation peaks to lower potential was observed (Fig. 4). The HOMO energy level can be obtained by following the procedure

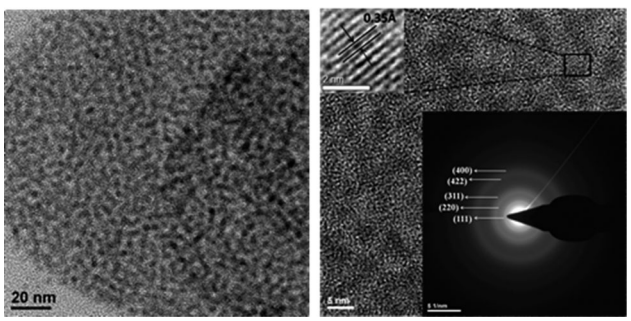

Fig. 2 HR-TEM images of CdSe QDs distribution (left) and lattice fringes (right). Inset: selected area electron diffraction.

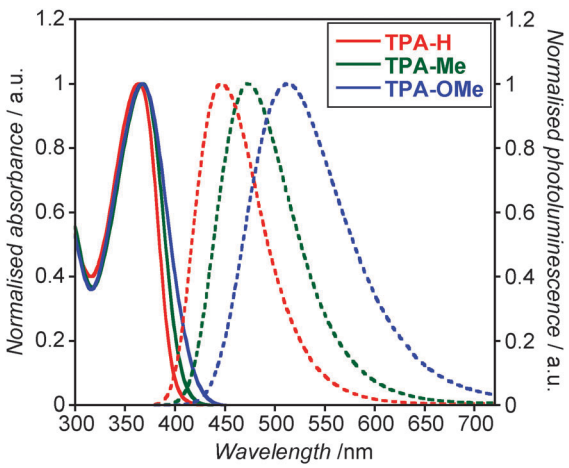

Fig. 3 Normalised UV-Visible absorption (solid line) and photoluminescence (dashed line) of **TPA-H** (red), **TPA-Me** (green) and **TPA-OMe** (blue) in CH_2Cl_2. Excitation at 365 nm.

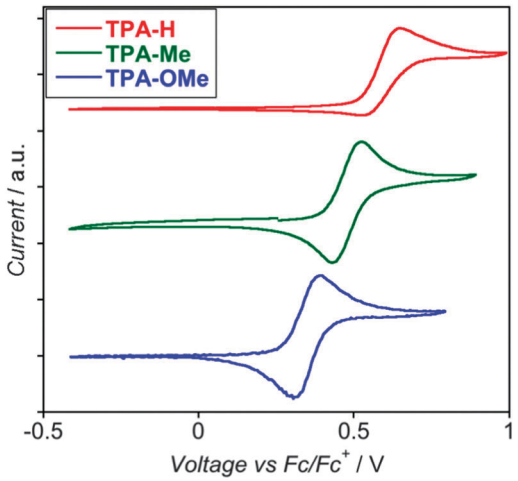

Fig. 4 Cyclic voltammetry traces of **TPA-H** (red), **TPA-Me** (green) and **TPA-OMe** (blue) acquired in CH_2Cl_2 solution containing 0.1 M [TBA][PF_6] and referenced to ferrocene. A scan rate of 50 mV s^{-1} was used.

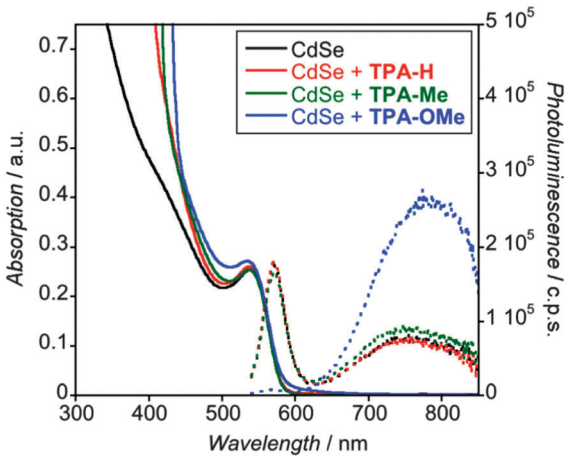

Fig. 5 UV-Visible absorption (solid line) and photoluminescence emission (dashed line) of pristine CdSe QDs (black) and its mixtures with **TPA-H** (red), **TPA-Me** (green) and **TPA-OMe** (blue). Excitation was at 530 nm.

described by Thompson *et al.* for fully reversible electrochemical process (Table 1).[11] It is worth highlighting that the TPA derivatives **TPA-Me** and **TPA-OMe** show reversible electrochemical behaviour (Fig. 4) evidenced by cyclic voltammetry at different scan rates (ESI†), therefore ensuring both the ability to extract or capture the hole from QDs, and also the subsequent hole transfer without any degradation. **TPA-H** shows some chemical-irreversibility at low scan rate but at higher scan rates this oxidation also appears to be fully reversible suggesting any degradation of the oxidised species is slow.

Having studied the properties of the isolated molecules, ligand exchange was performed through spontaneous de-protection of the thiol by mixing 1 mM of TPA in a dilute solution of CdSe QDs (63 μg ml^{-1}) in toluene at 70 °C for 16 hours under inert atmosphere.[12,13] Note that ligand exchange was not attained by using either TPA at μM concentration or shorter reaction times (1–2 hours). By knowing the average CdSe QD radius (thus volume) and using the bulk CdSe density, we are able to calculate the molar ratio between TPA and QDs, showing that approximately 6000-fold TPA per QD is necessary for an efficient ligand exchange. The pristine CdSe QDs show a characteristic excitonic peak at 535 nm and a sharp emission band centred at 570 nm (Fig. 5). Also observable is a broad emission band centred at 760 nm attributed to trap emission as is commonly observed.[14] As can be seen in Fig. 5, the high concentration of TPA used saturates the absorption at wavelengths below 400 nm, but the QDs excitonic peak intensity remains unaffected. Steady-state emission spectroscopy shows identical behaviour between the pristine CdSe QDs and those that have undergone ligand exchange with **TPA-H** or **TPA-Me**. However, the QDs excitonic emission is effectively quenched upon exchange with **TPA-OMe** suggesting hole transfer from the nanocrystal to the TPA derivative is occurring, a supposition consistent with the concomitant increase in trap emission observed.[14] The photogenerated holes on the CdSe undergo hole transfer to the **TPA-OMe** molecule attached to the surface thus reducing the QDs excitonic emission intensity. These holes can then recombine radiatively at trap sites located at the surface of the QDs. A control experiment using spiro-OMeTAD (a well-known hole transport material but without a thiol-based binding group) was also performed, and this showed no interaction with CdSe QDs.

To study this quenching of the QDs excitonic emission by the **TPA-OMe** hole extractor we performed a time-resolved PL experiment. The results of this are plotted in Fig. 6 using an excitation wavelength of 467 nm and thus almost exclusively exciting the QDs and not the TPA derivative. The data monitor the excitonic emission of the QDs (572 nm) and show that not only does the **TPA-OMe** hole extractor quench the QDs excitonic emission efficiently and thus support the steady-state PL data, but also that it quenches it quickly as has been observed by others. Within 10 ns, the emission intensity in the **TPA-OMe** capped QDs reduces by roughly a factor of 100 compared to its original value, whereas the intensity in the non-exchanged QDs at this point remains almost an order of magnitude larger.

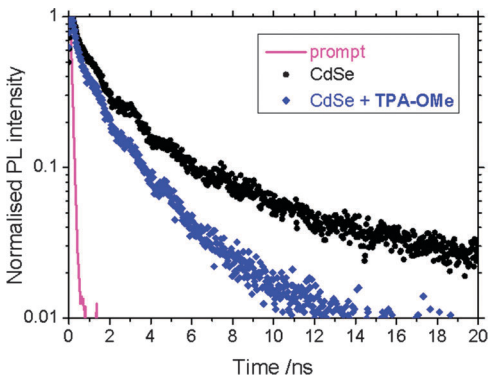

Fig. 6 Normalised transient photoluminescence data for pristine CdSe QDs (black) and its mixture with **TPA-OMe** (blue). Excitation was at 467 nm, and the band edge emission monitored at 572 nm. Also shown (magenta) is the instrument response of ~250 ps FWHM. Data with **TPA-H** and **TPA-Me** show longer lifetimes than **TPA-OMe** and are omitted for clarity. Multi-exponential fits are shown in the ESI.†

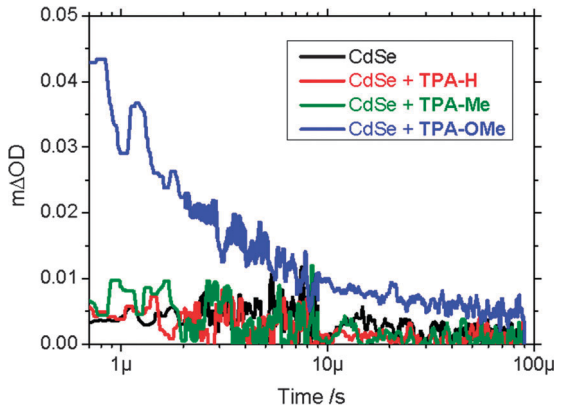

Fig. 7 Transient absorption kinetics of pristine CdSe QDs (black) and its mixtures with **TPA-H** (red), **TPA-Me** (green), and **TPA-OMe** (blue). Excitation was performed at 550 nm with an energy of 11.5 ± 1 μJ cm^{-2} and the absorption was probed at 900 nm.

Given that the LUMO of the TPA derivative lies substantially closer to vacuum than that of the QDs, both energy and electron transfer from the QDs to the TPA derivative are unlikely, and thus this fast quenching is most likely to be due to HOMO–HOMO hole transfer from the QDs to the **TPA-OMe** ligand.

In order to further probe this hole transfer process at the QD-hole extractor interface, we performed transient absorption spectroscopy to observe long-lived photogenerated products. These data are presented in Fig. 7 and show that when **TPA-OMe** is present an appreciable number of long-lived charges are generated upon optical excitation, a phenomenon that does not occur in the pristine CdSe QDs, or with the two other hole extractors. The transient spectrum of the **TPA-OMe** sample shows a broad peak centred around 850–900 nm, a feature we attribute to the **TPA-OMe** cation by comparison with the absorption spectrum of chemically oxidised **TPA-OMe** (ESI†). This normalised steady-state absorption spectrum of oxidised **TPA-OMe** in CH_2Cl_2 is obtained by chemically oxidising **TPA-OMe** with 1.1 equivalents of the chemical oxidant tris(4-bromophenyl)aminium hexachloroantimonate. The absorption spectrum of oxidised **TPA-OMe** accurately maps the transient spectrum at 1 μs, thus allowing the assignment of this feature in the transient absorption spectrum to oxidised **TPA-OMe** molecules. The decay of the absorption signal in Fig. 7 thus monitors the recombination of the electrons on the CdSe and the holes on the **TPA-OMe** ligand. These data are consistent with the steady-state and time-resolved PL quenching data and suggest that appreciable amounts of hole transfer are only occurring from the QDs to the **TPA-OMe** derivative, and not to either of the other ligands. The consequence of this hole transfer is consistent with an increased spatial separation between the electron on the CdSe and the hole on the ligand, resulting in the presence of long-lived decay phases with a timescale of a few microseconds.

Given that all of the data presented here were obtained from dilute solutions and thus on un-aggregated QDs, the spectroscopic differences between the ligands are likely to be due to energetic rather than morphological or aggregation effects. Thus we can rationalise the differing behaviour between the TPA derivatives by consideration of their respective HOMO energy levels. **TPA-OMe** has a HOMO level ~0.2 eV closer to vacuum than **TPA-Me** which is itself ~0.2 eV above that of **TPA-H**. It should be noted that DFT calculations of the reorganisation energy from each TPA derivative to its cation are all within 10 meV of each other and so can effectively be neglected (ESI†). Consequently, **TPA-OMe** is more readily oxidised than the other two hole extractors and so it is likely to be this energetic difference that gives rise to the photophysical properties observed; the **TPA-OMe** ligand simply presents a stronger driving force for hole transfer from the CdSe QDs. For **TPA-H** and **TPA-Me**, this lack of appreciable hole transfer from QDs, despite what appears to be a large driving force, is consistent with prior observations.[15] This discrepancy could be due to a range of factors such as the differing morphology of the TPA derivatives, and the presence of sub-bandgap hole traps within the QDs. These states can arise from intrinsic defects, such as metal vacancies,[16,17] and would reduce the apparent driving force available for hole transfer, necessitating a shallower HOMO level for efficient function.

3. Conclusions

We have reported the synthesis and characterisation of different triphenylamine-based hole capture materials for use with inorganic nanocrystals. When anchored to CdSe QDs these materials exhibit radically different performance dependent upon the position of their HOMO energy level. The most easily oxidised (**TPA-OMe**) displays hole extraction from the nanocrystal resulting in a reduced band edge PL intensity and lifetime, and the appearance of long-lived charges. We suggest that such materials could be used to reduce fast recombination in hybrid bulk heterojunction or nanocrystal-sensitized solar cells thus facilitating more facile long-lived charge generation. Work in this direction is underway.

4. Experimental

4.1. Synthetic procedure

Materials. All reagents were purchased from either Sigma-Aldrich or Alfa-Aesar and were used as received without further purification unless otherwise stated.

Synthesis of *S*-(4-iodophenyl) ethanethioate (1)[8]. A solution containing pipsyl chloride (5.13 g, 17 mmol); dimethylacetamide (4.65 ml, 50 mmol) in 20 ml of CH_2Cl_2 was added carefully to a suspension containing Zn powder (3.92 g, 60 mmol) dichlorodimethylsilane (7 ml, 58 mmol) in 20 ml of CH_2Cl_2. The mixture was stirred at 75 °C for 2 hours under N_2 atmosphere. The solution became clear, indicating that the reduction is accomplished. The mixture was brought to 40 °C and acetyl chloride (1.53 ml, 21.5 mmol) was added slowly. The mixture was stirred for an extra 15 minutes and cooled down to room temp. The crude was poured into 100 ml of water and extracted with 50 ml of CH_2Cl_2 twice. The organic layers were combined, dried over Na_2SO_4 and filtered off. The crude was purified by column chromatography (SiO_2, hexanes up to hexanes–CH_2Cl_2 4 : 1) to afford the product as white solid (3.2 g, 83% yield).

^{1}H NMR (500 MHz, $CDCl_3$) δ_H: 7.74 (d, J = 8.5 Hz, 2H); 7.13 (d, J = 8.5 Hz, 2H); 2.42 (s, 3H). ^{13}C NMR (125 MHz, $CDCl_3$) δ_C: 193.4; 138.6; 136.2; 128.0; 96.2; 30.5. MS EI (m/z): $[M]^+$ calcd for C_8H_7IOS: 277.92570; found: 277.92565. Anal. calcd for C_8H_7IOS: C, 34.55; H, 2.54; found: C, 34.64; H, 2.57.

Synthesis of *S*-(4-((4-(diphenylamino)phenyl)ethynyl)phenyl) ethanethioate (TPA-H). **1** (278 mg, 1 mmol), **2** (296 mg, 1.1 mmol), $(PPh_3)_2PdCl_2$ (70 mg, 0.1 mmol) and CuI (10 mg, 0.05 mmol) were place in a Schlenk tube and dried under high vacuum for 30 minutes. Then, a previously degassed solution of triethylamine (0.5 ml) in dry THF (5 ml) was added *via* cannula. The mixture was degassed again by the pump–freeze technique and stirred at 70 °C overnight under N_2. Then, a silica plug was run in CH_2Cl_2 and the solvent removed. The crude was purified by column chromatography (SiO_2, hexanes–$CHCl_3$ 2 : 1 up to 1 : 1) to afford the product as yellow oil which solidify slowly (288 mg, 68% yield). ^{1}H NMR (500 MHz, $CDCl_3$) δ_H: 7.52 (d, J = 8.4 Hz, 2H); 7.37 (m, 4H); 7.28 (m, 4H); 7.12 (d, J = 7.7 Hz, 4H); 7.07 (t, J = 7.5 Hz, 2H); 7.01 (d, J = 8.8 Hz, 2H); 2.43 (s, 3H). ^{13}C NMR (125 MHz, $CDCl_3$) δ_C: 193.8; 148.4; 134.4; 132.8; 132.2; 129.6; 127.7; 127.2; 125.3; 125.2; 123.8; 122.4; 115.8; 91.7; 88.1; 30.5. MS EI (m/z): $[M]^+$ calcd for $C_{28}H_{21}NOS$: 419.13384; found: 419.133932. Anal. calcd for $C_{28}H_{21}NOS$: C, 80.16; H, 5.05; N, 3.34; found: C, 80.02; H, 4.94; N, 3.17.

Synthesis of *S*-(4-((4-(di-*p*-tolylamino)phenyl)ethynyl)phenyl) ethanethioate (TPA-Me). **1** (550 mg, 2.35 mmol), **3** (700 mg, 2.35 mmol), $(PPh_3)_2PdCl_2$ (165 mg, 0.24 mmol) and CuI (23 mg, 0.12 mmol) were place in a Schlenk tube and dried under high vacuum for 30 minutes. Then, a previously degassed solution of triethylamine (1.2 ml) in dry THF (12 ml) was added *via* cannula. The mixture was degassed again by the pump–freeze technique and stirred at 70 °C overnight under N_2. Then, a silica plug was run in CH_2Cl_2 and the solvent removed. The crude was purified by column chromatography (SiO_2, hexanes–$CHCl_3$ 4 : 1 up to 1 : 1) to afford the product as yellow solid (371 mg, 36% yield). ^{1}H NMR (500 MHz, $CDCl_3$) δ_H: 7.52 (d, J = 8.1 Hz, 2H); 7.37 (d, J = 8.3 Hz, 2H); 7.33 (d, J = 8.7 Hz, 2H); 7.09 (d, J = 8.01 Hz, 4H); 7.01 (d, J = 8.4 Hz, 4H); 6.94 (d, J = 8.9 Hz, 2H); 2.42 (s, 3H); 2.32 (s, 6H). ^{13}C NMR (125 MHz, $CDCl_3$) δ_C: 193.8; 148.7; 144.7; 134.4; 133.6; 132–7; 132.1; 130.2; 127.5; 125.5; 125.3; 121.1; 114.6; 91.9; 87.8; 30.4; 21.1. MS EI (m/z): $[M]^+$ calcd for $C_{30}H_{25}NOS$: 447.16514; found: 447.165272. Anal. calcd for $C_{30}H_{25}NOS$: C, 80.50; H, 5.63; N, 3.13; found: C, 80.40; H, 5.53; N, 3.08.

Synthesis of *S*-(4-((4-(bis(4-methoxyphenyl)amino)phenyl)-ethynyl)phenyl) ethanethioate (TPA-OMe). **1** (425 mg, 1.53 mmol), **4** (544 mg, 1.68 mmol), $(PPh_3)_2PdCl_2$ (107 mg, 0.16 mmol) and CuI (15 mg, 0.08 mmol) were place in a Schlenk tube and dried under high vacuum for 30 minutes. Then, a previously degassed solution of triethylamine (0.8 ml) in dry THF (8 ml) was added *via* cannula. The mixture was degassed again by the pump–freeze technique and stirred at 70 °C overnight under N_2. Then, a silica plug was run in CH_2Cl_2 and the solvent removed. The crude was purified by column chromatography (SiO_2, hexanes–CH_2Cl_2 2 : 1 up to 1 : 1) to afford the product as yellow solid (567 mg, 77% yield). ^{1}H NMR (500 MHz, $CDCl_3$) δ_H: 7.51 (d, J = 8.3 Hz, 2H); 7.36 (d, J = 8.3 Hz, 2H); 7.30 (d, J = 8.8 Hz, 2H); 7.07 (m, 4H); 6.84 (m, 6H); 3.80 (s, 6H); 2.42 (s, 3H). ^{13}C NMR (125 MHz, $CDCl_3$) δ_C: 193.0; 156.6; 149.2; 140.3; 134.4; 132.7; 132.1; 127.6; 127.4; 125.4; 119.4; 119.3; 115.0; 113.6; 92.1; 87.6; 55.7; 30.5. MS EI (m/z): $[M]^+$ calcd for $C_{30}H_{25}NO_3S$: 479.15486; found: 479.15497. Anal. calcd for $C_{30}H_{25}NO_3S$: C, 75.13; H, 5.25; N, 2.92; found: C, 75.18; H, 5.18; N, 2.85.

Synthesis of CdSe quantum dots. The oleic acid caped CdSe quantum dots were synthesized using a previously reported method with some modifications.[18] The synthetic process was carried out by the hot injection method. Trioctylphosphine selenide (TOPSe) precursor was synthesized by mixing 4 mM selenium powder and 5 ml trioctylphosphine (TOP) dissolved in 5 ml of 1-octadecene in an argon atmosphere. Separately, 0.51 mg of cadmium oxide was placed in a three-necked round bottle flask with a mixture of 1-octadecene (25 ml) and oleic acid (5 ml). This was heated at 240 °C under an argon atmosphere for one hour. TOPSe solution was quickly injected into the above mixture at 240 °C and the temperature was kept constant for 90 seconds. Afterwards, the heater was removed and the solution was allowed to cool. Precipitation of the red coloured CdSe quantum dots was achieved by adding absolute ethanol solution. CdSe particles were finally isolated by centrifugation. Purification of CdSe quantum dots was obtained by dissolving in toluene and with ethanol followed by centrifugation. The washing process was carried out five times and then finally the product was stored as a soluble dispersion in toluene.

4.2. Methods

Chemical characterisation. ^{1}H and ^{13}C NMR spectra were recorded on Bruker Advance 500 spectrometer (500 MHz for ^{1}H and 125 MHz for ^{13}C). The deuterated solvents are indicated; chemical shifts, δ, are given in ppm, referenced to the solvent residual signal (^{1}H, ^{13}C). MS were recorded on ThermoElectron MAT 900 using electron impact (EI) ionization technique. Elemental analyses were carried out by Stephen Boyer at London Metropolitan University using a Carlo Erba CE1108 Elemental Analyzer.

Nanoparticles characterisation. Powder X-ray diffraction data was collected using Philips X'Pert PRO apparatus. High-Resolution Transmission Electron Microscopy (HR-TEM) images were recorded by using FEI Tecnai300 apparatus.

Electrochemical characterisation. All cyclic voltammetry measurements were carried out in freshly distilled CH_2Cl_2 using 0.1 M [TBA][PF_6] electrolyte in a three-electrode system, with each solution being purged with N_2 prior to measurement. The working electrode was a Pt disk. The reference electrode was Ag/AgCl and the counter electrode was a Pt rod. All measurements were made at room temp. using an μAUTOLAB Type III potentiostat, driven by the electrochemical software GPES. Cyclic voltammetry (CV) measurements used scan rates of 25, 50, 100, 200 and 500 mV s^{-1}, and differential pulse voltammetry (DPV) was carried out at a step potential of 10 mV, modulation amplitude of 100 mV, modulation time of 0.05 s

and an interval time of 0.5 s, giving a scan rate of 20 mV s^{-1}. Ferrocene was used as internal standard in each measurement.

Steady-state optical characterisation. Solution-phase UV-Visible absorption spectra were recorded using Jasco V-670 UV/Vis/NIR spectrophotometer controlled using the SpectraManager software. Photoluminescence (PL) spectra were recorded with Fluoromax-3 fluorimeter controlled by the ISAMain software. All samples were measured in a 1 cm cell at room temp. with dichloromethane as a solvent. Concentration of 5×10^{-6} M was used for UV/Visible and PL.

Transient photoluminescence characterisation. Time-resolved photoluminescence data was collected by time-correlated single photon counting using a Horiba Jobin Yvon IBH Fluorocube. Excitation was performed with a photodiode operating at 1 MHz with an output of 467 nm at an average intensity of 80 μW cm^{-2}.

Transient absorption studies. Micro-second transient absorption spectroscopy was performed on solutions and all data shown is scaled for the fraction of photons absorbed at the excitation wavelength. The samples were excited by a dye laser (Photon Technology International Inc. GL-301) pumped by a nitrogen laser (Photon Technology International Inc. GL-3300) to give a pulse width of 0.6 ns at 4 Hz. Excitation was at 550 nm at an energy of 11.5 ± 1 μJ cm^{-2}. The samples were probed using a quartz halogen lamp (Bentham, IL1) with a stabilised power supply (Bentham, 605). The probe light was detected using a silicon or $In_xGa_{1-x}As$ photodiode and the signal subsequently amplified and passed through electronic band-pass filters to improve the signal to noise ratio.

Computational details. The molecular structures were optimized first in vacuum without any symmetry constrains, followed by the addition of solvent contribution *via* a conductor-like polarizable continuum model (C-PCM).[19] The presence of local minimum was confirmed by the absence of imaginary frequencies. All calculations were carried out using the Gaussian 09 programme[20] with the Becke three parameter hybrid exchange, Lee Yang-Parr correlation functional (B3LYP) level of theory. All atoms were described by the 6-31G(d) basis set. All structures were input and processed through Avogadro software package.[21]

Acknowledgements

We thank the Engineering and Physical Sciences Research Council (EPSRC - UK) and Department of Science & Technology (DST - India) APEX project for financial support. S.A.H would like to acknowledge support from the Royal Society through an award of a Royal Society University Research Fellowship.

Notes and references

1 H. M. Chen, C. K. Chen, Y.-C. Chang, C.-W. Tsai, R.-S. Liu, S.-F. Hu, W.-S. Chang and K.-H. Chen, *Angew. Chem., Int. Ed.*, 2010, **49**, 5966–5969.
2 X. Michalet, F. F. Pinaud, L. A. Bentolila, J. M. Tsay, S. Doose, J. J. Li, G. Sundaresan, A. M. Wu, S. S. Gambhir and S. Weiss, *Science*, 2005, **307**, 538–544.
3 J. Albero, Y. Zhou, M. Eck, F. Rauscher, P. Niyamakom, I. Dumsch, S. Allard, U. Scherf, M. Kruger and E. Palomares, *Chem. Sci.*, 2011, **2**, 2396–2401.
4 J. A. Chang, J. H. Rhee, S. H. Im, Y. H. Lee, H.-j. Kim, S. I. Seok, M. K. Nazeeruddin and M. Gratzel, *Nano Lett.*, 2010, **10**, 2609–2612.
5 F. T. F. O'Mahony, T. Lutz, N. Guijarro, R. Gomez and S. A. Haque, *Energy Environ. Sci.*, 2012, **5**, 9760–9764.
6 H.-S. Kim, C.-R. Lee, J.-H. Im, K.-B. Lee, T. Moehl, A. Marchioro, S.-J. Moon, R. Humphry-Baker, J.-H. Yum, J. E. Moser, M. Gratzel and N.-G. Park, *Sci. Rep.*, 2012, **2**, 591.
7 R. Karel Čapek, I. Moreels, K. Lambert, D. De Muynck, Q. Zhao, A. Van Tomme, F. Vanhaecke and Z. Hens, *J. Phys. Chem. C*, 2010, **114**, 6371–6376.
8 Z.-F. Shi, L.-J. Wang, H. Wang, X.-P. Cao and H.-L. Zhang, *Org. Lett.*, 2007, **9**, 595–598.
9 L. A. Estrada and D. C. Neckers, *Org. Lett.*, 2011, **13**, 3304–3307.
10 J.-S. Yang, S.-Y. Chiou and K.-L. Liau, *J. Am. Chem. Soc.*, 2002, **124**, 2518–2527.
11 B. W. D'Andrade, S. Datta, S. R. Forrest, P. Djurovich, E. Polikarpov and M. E. Thompson, *Org. Electron.*, 2005, **6**, 11–20.
12 I. S. Liu, H.-H. Lo, C.-T. Chien, Y.-Y. Lin, C.-W. Chen, Y.-F. Chen, W.-F. Su and S.-C. Liou, *J. Mater. Chem.*, 2008, **18**, 675–682.
13 J. Albero, E. Martinez-Ferrero, D. Iacopino, A. Vidal-Ferran and E. Palomares, *Phys. Chem. Chem. Phys.*, 2010, **12**, 13047–13051.
14 D. R. Baker and P. V. Kamat, *Langmuir*, 2010, **26**, 11272–11276.
15 H. C. Leventis, F. O'Mahony, J. Akhtar, M. Afzaal, P. O'Brien and S. A. Haque, *J. Am. Chem. Soc.*, 2010, **132**, 2743–2750.
16 E. Kuçur, W. Bücking, R. Giernoth and T. Nann, *J. Phys. Chem. B*, 2005, **109**, 20355–20360.
17 V. Babentsov and F. Sizov, *Opto-Electron. Rev.*, 2008, **16**, 208–225.
18 J. Chen, J. L. Song, X. W. Sun, W. Q. Deng, C. Y. Jiang, W. Lei, J. H. Huang and R. S. Liu, *Appl. Phys. Lett.*, 2009, **94**, 153115.
19 M. Cossi, N. Rega, G. Scalmani and V. Barone, *J. Comput. Chem.*, 2003, **24**, 669–681.
20 M. J. Frisch, *et al.*, *Gaussian 09, Revision A.1*, Gaussian Inc., Wallingford, USA, 2009.
21 M. D. Hanwell, D. E. Curtis, D. C. Lonie, T. Vendermeersch, E. Zurek and G. R. Hutchinson, *J. Cheminf.*, 2012, **4**, 17.
22 C. Querner, P. Reiss, S. Sadki, M. Zagorska and A. Pron, *Phys. Chem. Chem. Phys.*, 2005, **7**, 3204–3209.

